


 Cite this: *Nanoscale*, 2022, **14**, 9754

A family of superconducting boron crystals made of stacked bilayer borophenes†

 Yuewen Mu,  *^a Bao-Tian Wang,  ^b Si-Dian Li  *^c and Feng Ding*^d

Monolayer borophenes tend to be easily oxidized, while thicker borophenes have stronger antioxidation properties. Herein, we proposed four novel metallic boron crystals by stacking the experimentally synthesized borophenes, and one of the crystals has been reported in our previous experiments. Bilayer units tend to act as blocks for crystals as determined by bonding analyses. Their kinetic, thermodynamic and mechanical stabilities are confirmed by our calculated phonon spectra, molecular dynamics and elastic constants. Our proposed allotropes are more stable than the boron α -Ga phase below 1000 K at ambient pressure. Some of them become more stable than the α -rh or γ -B₂₈ phases at appropriate external pressure. More importantly, our calculations show that three of the proposed crystals are phonon-mediated superconductors with critical temperatures of about 5–10 K, higher than those of most superconducting elemental solids, in contrast to typical boron crystals with significant band gaps. Our study indicates a novel preparation method for metallic and superconducting boron crystals dispensing with high pressure.

 Received 12th April 2022,
Accepted 2nd June 2022

DOI: 10.1039/d2nr02013k

rsc.li/nanoscale

1. Introduction

Boron presents several complex crystal allotropes due to its unique multi-center bonding as a result of its electron-deficient nature. At normal pressure, boron has three typical crystal allotropes: α rhombohedral (α -rh),¹ β rhombohedral (β -rh)² and β tetragonal (β -t) phases.³ There is also a high-pressure orthorhombic phase (γ -B₂₈).⁴ Generally speaking, all these boron crystals are composed of B₁₂ icosahedrons and boron monomers/dimers, which leads to semiconducting behavior with significant band gaps.^{5–7}

In contrast to the semiconducting behavior of boron crystals, boron nanomaterials (*e.g.*, boron nanotubes and monolayers) behave quite differently. Almost all the single-walled boron nanotubes preferably exhibit metallic behavior unless curvature-induced buckling of certain atoms opens gaps for very narrow nanotubes.^{8,9} It is quite different from the chirality-dependent transport behaviors in single-walled carbon nanotubes. As for boron monolayers (referred to as borophenes¹⁰), whether they are already prepared (*e.g.*, β ₁₂,¹¹ χ ₃¹¹ or honeycomb δ ₃¹²) or only theoretically predicted,^{13–15} they also preferably exhibit metallic behavior unless connected network of hexagonal vacancies opens the gaps.¹⁶ Borophenes have drawn a lot of attention due to their promising applications in batteries,¹⁷ high-speed electronic devices,^{18,19} flexible devices,²⁰ water splitting,²¹ and so on.²²

As is well known, graphite could serve as the precursor of graphene in the process of mechanical exfoliation,²³ while in the reverse process, graphene could be stacked into graphite. In contrast, there is no layered phase for boron crystals due to severe electron deficiency. Thus mechanical exfoliation fails for borophenes. Monolayer borophenes were successfully prepared on silver,^{11,24} copper,²⁵ aluminum²⁵ and gold²⁶ substrates by the molecular beam epitaxy (MBE) method. Very recently, borophene concentric superlattices²⁷ and bilayer borophenes^{28–30} were also experimentally realized, and the borophene island shapes could be controlled by the growth temperature and deposition rate.³¹ However, monolayer borophenes tend to be easily oxidized,^{32,33} while the thicker borophene has stronger antioxidation properties.²⁸ What would

^aKey Laboratory of Materials for Energy Conversion and Storage of Shanxi Province, Institute of Molecular Science, Shanxi University, Taiyuan, 030006, China. E-mail: ywmu@sxu.edu.cn

^bSpallation Neutron Source Science Center, Institute of High Energy Physics, Chinese Academy of Sciences (CAS), Dongguan, Guangdong 523803, China

^cKey Laboratory of Materials for Energy Conversion and Storage of Shanxi Province, Institute of Molecular Science, Shanxi University, Taiyuan, 030006, China. E-mail: lisdian@sxu.edu.cn

^dCentre for Multidimensional Carbon Materials, Institute for Basic Science, Ulsan, South Korea. E-mail: f.ding@unist.ac.kr

†Electronic supplementary information (ESI) available: Table of *k*-mesh, *q*-mesh, EPC constants and superconducting critical temperatures; primitive cells and corresponding Brillouin zones and high-symmetry *k*-points; phase transition of bilayer borophene; phonon spectra using Phonopy; BOMD simulations with RMSD; high-pressure phases of α -B₁₆ and δ ₆-B₆ allotropes; table of main elastic constants; projected density of states; phonon spectrum with electron-phonon coupling modes; and SSADNDP and ELF. See DOI: <https://doi.org/10.1039/d2nr02013k>

happen when much more boron atoms are deposited onto the borophenes, especially when stacking borophenes into thick films or even crystals like graphite or B₂O₃ polymorphs?³⁴

In this paper, we proposed four novel metallic three dimensional (3D) boron allotropes through stacking the experimentally reported borophenes. It should be pointed out that one of the crystals has been experimentally realized and acts as efficient electrocatalysts for lithium–sulfur batteries.³⁵ Their kinetic, thermodynamic and mechanical stabilities were confirmed by our calculated phonon spectra, molecular dynamics and elastic constants. As is well known, high pressure is required for the nonmetal–metal transition in the boron solid. For example, α -rh boron would transform into the metallic α -Ga phase at 74 GPa from the thermodynamic point of view;³⁶ however, much higher pressure would be required due to the high energy barriers for the destruction of tightly bonded B₁₂ clusters.³⁷ Our results indicate a novel preparation method for metallic boron crystals dispensing with high pressure.

2. Methods

All the calculations except superconducting properties were carried out using the Vienna *ab initio* simulation package (VASP 5.4)^{38,39} with the projector augmented wave (PAW) pseudopotential method^{40,41} and Perdew–Burke–Ernzerhof (PBE) functional.⁴² Both lattice parameters and atomic positions were optimized using the conjugate gradient method, and the convergence criteria for energy and force were 1×10^{-6} eV and 1×10^{-3} eV Å⁻¹, respectively. The kinetic energy cutoff for plane waves was set to 450 eV. A large vacuum spacing (more than 15 Å) was taken to prevent mirror interactions. The Brillouin zones were sampled with $2\pi \times 0.02$ Å⁻¹ spacing in the reciprocal space by the Monkhorst–Pack scheme.⁴³ The primitive cells and the corresponding high symmetry K-points for the band structure, phonon dispersion and density of states (DOS) were generated using the AFLOW package.⁴⁴ Grimme's DFT-D3 van der Waals (vdW) corrections with the Becke–Jonson (BJ) damping^{45,46} was employed. Due to the well-known underestimation of band gaps by Kohn–Sham DFT methods, the Heyd–Scuseria–Ernzerhof (HSE06)⁴⁷ screened hybrid functional was employed for more accurate band structures. The phonon spectra were calculated by the density-functional perturbation theory (DFPT) method implemented in the Phonopy program⁴⁸ interfaced with VASP. The Born–Oppenheimer molecular dynamics (BOMD) simulations were carried out with Nose–Hoover thermostat in the canonical ensemble (NVT), the timestep for which was 1 fs. The crystal structures and the charge densities were visualized using the VESTA package.⁴⁹ The X-ray diffraction (XRD) patterns were simulated using wavelengths of 1.54059 Å and 1.54432 Å (relative intensities 1 : 0.5) using the VESTA package.⁴⁹ The Elastic constants were calculated using the VASP package, and the bulk modulus B and shear modulus G were defined using the Voigt–Reuss–Hill approximations.⁵⁰

The superconducting properties were calculated based on Bardeen–Cooper–Schrieffer (BSC) theory⁵¹ and Migdal–Eliashberg theory^{52,53} implemented in the Quantum ESPRESSO package.^{54,55} The Perdew–Burke–Ernzerhof (PBE) functional⁴² and optimized norm-conserving Vanderbilt pseudopotentials (ONCVSP)⁵⁶ were employed. And 70 Ry and 280 Ry were used for the wavefunction and charge density cutoffs, the same as those used in the previous superconductor calculation for borophenes.¹⁹ Methfessel–Paxton smearing with a width of 0.02 Ry was used for the self-consistent calculations.¹⁹ Both lattice parameters and atomic positions were reoptimized before superconductor calculations. The k -meshes and q -meshes for phonon (PH) and electron–phonon coupling (EPC) are listed in Table S1.†

3. Results and discussion

Due to multi-center bonding, the borophene has a lot of allotropes with nearly degenerate energies, no matter whether they are in freestanding form^{14,15,60} or attached to a support.^{61,62} In this study, we considered the stacking of four types of borophenes with different hole densities (*i.e.*, $\eta = 0, 1/9, 1/6$ and $1/3$ for triangular δ_6 , α , β_{12} and honeycomb δ_3 borophenes, respectively), which have been already prepared on Ag(111) or Al(111) substrates in experiments.^{11,12,24,63} Two layers of these borophenes were stacked vertically in several modes like in graphite, and fully relaxed. The most stable ones were selected for further study, and the precursor layers were colored in red and purple, as shown in Fig. 1.

Fig. 1 shows four 3D boron allotropes derived from the staking of δ_6 , α , β_{12} and δ_3 borophenes. We use “Name_{2D}-B_{*n*}” to distinguish the allotropes, where Name_{2D} is the name of the precursor 2D borophene,¹³ and n is the number of boron atoms in the primitive cell. According to this definition, the four allotropes are named δ_6 -B₆, α -B₁₆, β_{12} -B₅ and δ_3 -B₄, the space groups for which are $C2/m$, $C2/m$, $P\bar{6}m2$ and $C2/m$, respectively. Their lattice parameters and Wyckoff positions for their conventional cells are listed in Table 1 and Fig. 1. Besides, the data of α -rh, γ -B₂₈ and α -Ga phases are also listed for comparison. Meanwhile, the primitive cells of the proposed allotropes generated by the AFLOW package⁴⁴ are displayed in Fig. S1† and used for further calculations. Interestingly, bilayer borophenes with strong inter-layer bonding and buckled atoms (red and pink layers in Fig. 1) tend to act as building blocks of 3D crystals, and their inter-layer distances are smaller than those between bilayers (to be discussed in detail later). They are similar to boron double chains, which act like carbon single chains to balance the intrinsic electron deficiency of boron atoms.⁶⁴ The bilayer units in β_{12} -B₅ and δ_3 -B₄ showed much larger deformation than their freestanding forms,⁶⁵ especially β_{12} -B₅ had a hexagonal primitive cell (Fig. 1c and Fig. S1c†) as reported in our previous experimental study.³⁵ The phase transition from the free-standing bilayer β_{12} borophene⁶⁵ to the β_{12} -B₅ bilayer unit was investigated using the solid state nudged elastic band (SS-NEB) method.⁶⁶ It

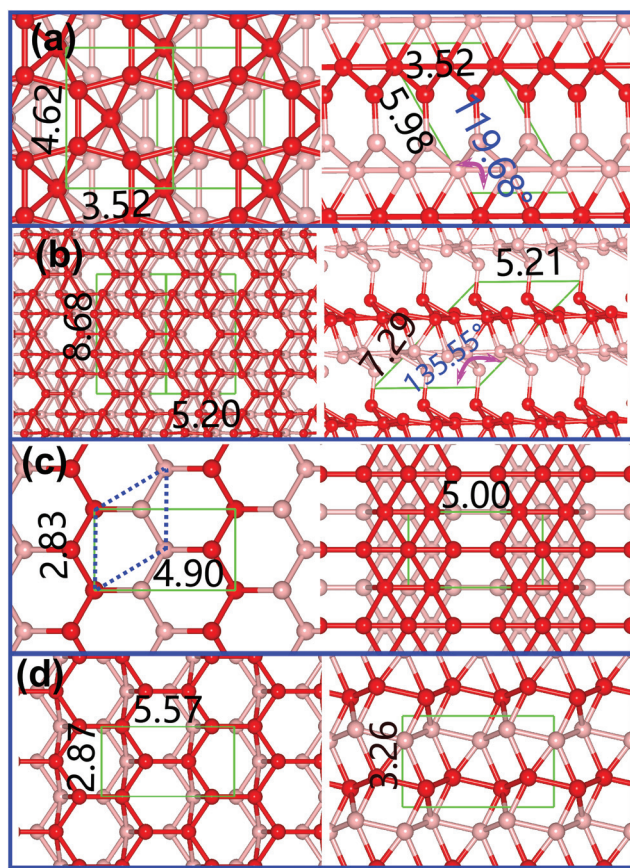


Fig. 1 Top and side views of the proposed allotropes (a) $\delta_6\text{-B}_6$, (b) $\alpha\text{-B}_{16}$, (c) $\beta_{12}\text{-B}_5$ and (d) $\delta_3\text{-B}_4$ with conventional cells. The lattice parameters are labeled in Å. The precursor layers are colored in red and purple.

showed that a barrier of 1.62 eV had to be overcome (as shown in Fig. S3†), though they were almost degenerate in energy. However, the barrier for multilayers may decrease as a result of enhanced stability and synergetic effect. Besides, high preparation temperature would also promote the transition.

The densities of $\delta_6\text{-B}_6$, $\alpha\text{-B}_{16}$ and $\beta_{12}\text{-B}_5$ allotropes are close to the value of $\alpha\text{-rh}$, while the density of $\delta_3\text{-B}_4$ is close to that of the $\alpha\text{-Ga}$ phase. The Vickers hardness is estimated using an empirical model $H_v = 2.0(\kappa^2 G)^{0.585} - 3.0$,⁶⁷ where $\kappa = G/B$, B , and G are Pugh's modulus ratio, bulk modulus and shear modulus in Voigt–Reuss–Hill (VRH) approximation,⁵⁰ respectively. The calculated Vickers hardnesses (Table 1) for $\alpha\text{-rh}$ and $\gamma\text{-B}_{28}$ are very close to their experimental values,^{57,58} which confirmed the reliability of our calculations. The Vickers hardnesses of our four proposed allotropes, especially $\alpha\text{-B}_{16}$, indicate that they are much softer than $\alpha\text{-rh}$ and $\gamma\text{-B}_{28}$ phases. According to the Pugh rules⁶⁸ and Frantsevich rules,⁶⁹ our proposed allotropes and other allotropes are all categorized as brittle materials because their Pugh's modulus ratio and Poisson's ratio are smaller than 1.75 and 0.33, respectively (Table S2†); meanwhile, our proposed allotropes are much more ductile than other boron allotropes.

Then we focused on the stabilities of the proposed allotropes. The average binding energy is defined as $E_b = (N \times E_B - E_{3D})/N$, where E_B and E_{3D} are the energies of an isolated boron atom in a vacuum and the 3D allotrope, and N is the number of boron atoms in the unit cell. The average binding energies of the proposed allotropes are 6.35–6.40 eV at the PBE + D3 level, which are a little smaller than those of $\alpha\text{-rh}$ (6.57 eV) and $\gamma\text{-B}_{28}$ (6.46 eV). But they are larger than those of the $\alpha\text{-Ga}$ phase (6.33 eV), which was supposed to be the high-pressure boron metallic phase in experiments.^{5,36} Furthermore, their stabilities were examined by phonon calculations and Born–

Table 1 The space group, lattice parameters (Å), Wyckoff positions, average binding energy E_b (eV), density ρ (g cm^{-3}), Vickers hardness H_v (GPa), Debye temperature θ_D (K) and superconducting critical temperatures T_c (K) for the proposed allotropes, $\alpha\text{-Ga}$, $\alpha\text{-rh}$ and $\gamma\text{-B}_{28}$ phases

Allotrope	Space group	Lattice parameters	Wyckoff positions	E_b	ρ	H_v	θ_D	T_c
$\delta_6\text{-B}_6$	$C2/m$	$a = 3.515$ $b = 4.617$ $c = 5.976$ $\beta = 119.683^\circ$	$8j$ (0.478, 0.801, 0.844) $4i$ (0.627, 0.000, 0.661)	6.39	2.56	29.50	1472.54	10.15
$\alpha\text{-B}_{16}$	$C2/m$	$a = 5.205$ $b = 8.679$ $c = 7.291$ $\beta = 135.545^\circ$	$8j$ (0.572, 0.839, 0.671) $8j$ (0.382, 0.675, 0.660) $8j$ (0.853, 0.333, 0.836) $4i$ (0.547, 0.500, 0.649) $4i$ (0.917, 0.500, 0.702)	6.35	2.49	16.92	1215.69	—
$\beta_{12}\text{-B}_5$	$P\bar{6}m2$	$a = 2.828$ $b = 2.828$ $c = 5.003$ $\gamma = 120^\circ$	$2g$ (0.000, 0.000, 0.174) $2h$ (0.333, 0.667, 0.333) $1c$ (0.333, 0.667, 0.000)	6.40	2.59	32.08	1506.58	9.36
$\delta_3\text{-B}_4$	$C2/m$	$a = 5.573$ $b = 2.869$ $c = 3.259$	$4i$ (0.768, 0.000, 0.826) $4i$ (0.592, 0.500, 0.703)	6.37	2.76	24.86	1426.82	5.65
$\alpha\text{-Ga}$ ³⁶	$Cmce^a$	—	—	6.33	2.88	59.38	1815.10	—
$\alpha\text{-rh}$ ¹	$R\bar{3}m$	—	—	6.57	2.53	37.02 ^b	1532.54 ^c	—
$\gamma\text{-B}_{28}$ ⁴	$Pnnm$	—	—	6.46	2.58	49.34 ^b	1640.85	—

^a Space group $Cmce$ used to be referred to as $Cmca$. ^b The experimental hardnesses for $\alpha\text{-rh}$ and $\gamma\text{-B}_{28}$ phases are 42 GPa (ref. 57) and 50 GPa,⁵⁸ respectively. ^c The experimental Debye temperature for $\alpha\text{-rh}$ phase is 1430 K.⁵⁹

Oppenheimer molecular dynamics (BOMD) simulations. As shown in Fig. S4 and S5,[†] the proposed allotropes are all kinetically stable as evidenced by the absence of any negative frequency in the entire Brillouin zone. All the three acoustic branches for the proposed allotropes are linearly dispersed near the Γ point, indicating strong covalent bonds between boron atoms in the three directions. The root mean square deviations (RMSD) for the proposed allotropes are very small (~ 0.2 Å) in the BOMD simulations (Fig. S5[†]), which suggests that all the proposed allotropes are able to withstand high temperatures up to 1000 K without any obvious structural reconstruction. It confirms these allotropes are separated by high barriers from other minima on the potential energy surface. Finally, the mechanical stability criteria^{70,71} for the four proposed allotropes are all satisfied (Table S2[†]), which suggests that they are mechanically stable. The Debye temperatures for the allotropes are calculated from elastic constants⁷² as follows,

$$\theta_D = \frac{h}{k_B} \left[\frac{3n N_A \rho}{4\pi M} \right]^{\frac{1}{3}} \left[\frac{2}{3} \left(\frac{\rho}{G} \right)^{\frac{2}{3}} + \frac{1}{3} \left(\frac{\rho}{B + 4G/3} \right)^{\frac{2}{3}} \right]^{\frac{3}{2}}$$

where h , k_B and N_A are Planck's constant, the Boltzmann constant and Avogadro's number, respectively, M is the molecular weight of the solid and $n = 1$ is the number of atoms in the molecule. As shown in Table 1, the calculated Debye temperature for α -rh agreed well with the experimental one (1430 K (ref. 59)), and all the proposed allotropes except α -B₁₆ have very high Debye temperatures (~ 1500 K), indicating strong bonding in these allotropes.

The free energies for the allotropes were also evaluated using the quasiharmonic approximation (QHA) method implemented in the Phonopy program.⁴⁸ They were calculated from 0 to 1000 K at ambient pressure as follows,

$$F = U(V_0) + \frac{1}{2} \sum_{qv} \hbar \omega_{qv} + k_B T \sum_{qv} \ln [1 - \exp(-\hbar \omega_{qv}/k_B T)],$$

where $U(V_0)$ is the ground state energy at the relaxed volume V_0 , T is temperature, and ω_{qv} is the phonon frequency for the band ν at wave vector q . The free energies from the contribution of electronic excitations⁷³ of α -Ga and the proposed allotropes were evaluated, and it was found that they were smaller than 2 meV per atom below 1000 K, so they were neglected in the calculations. As shown in Fig. 2a, the relative stabilities of the proposed allotropes, α -Ga, α -rh and γ -B₂₈ do not change, in other words, our proposed allotropes remain more stable than the α -Ga phase up to 1000 K. The effect of pressure on the stabilities of the allotropes were also evaluated by calculating the enthalpies of relaxed structures under different pressures (Fig. 2b). The proposed allotropes δ_3 -B₄, δ_6 -B₆ and α -B₁₆ become more stable than the α -rh phase above 63, 155 and 173 GPa, respectively, though phase transition occurs for δ_6 -B₆ and α -B₁₆ phases at high pressure (Fig. S6[†]). Our predicted transition pressures from α -rh to γ -B₂₈ and from

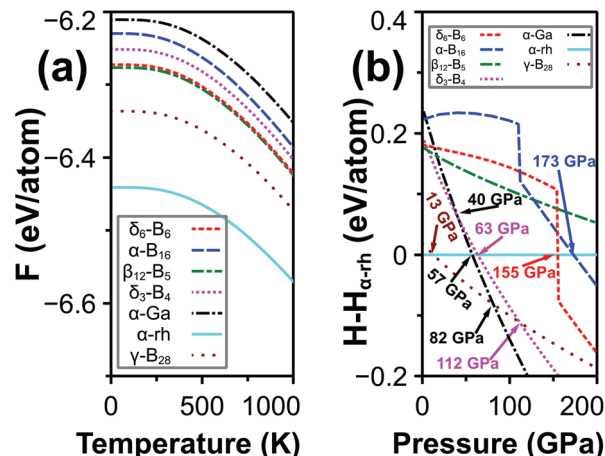


Fig. 2 (a) Free energies of the proposed allotropes, α -Ga, α -rh and γ -B₂₈ phases as a function of temperature at ambient pressure and (b) enthalpies of the proposed allotropes, α -Ga, α -rh and γ -B₂₈ phases relative to α -rh as a function of pressure.

γ -B₂₈ to α -Ga are 13 and 82 GPa at the PBE + D3 level, respectively, agreeing well with previous calculations (19 and 89 GPa at the PBE level, respectively).⁵ The δ_3 -B₄ allotrope remains more stable than the α -Ga phase below 40 GPa, and becomes more stable than β -rh and T-192 phases above this pressure.⁵ It should be pointed out that all the transition pressures were predicted from a thermodynamic perspective, which would be delayed when considering kinetic factors, such as the destruction of strong covalent bonds.³⁶

Different electronic properties are expected compared to typical boron crystals due to the absence of B₁₂ icosahedrons. As shown in Fig. 3, many bands (at PBE and HSE06 levels) are crossed by the Fermi level, which suggests they are metallic, further confirmed by the non-zero density of states (DOS) at the Fermi level (Fig. S7[†]). They are quite different from typical

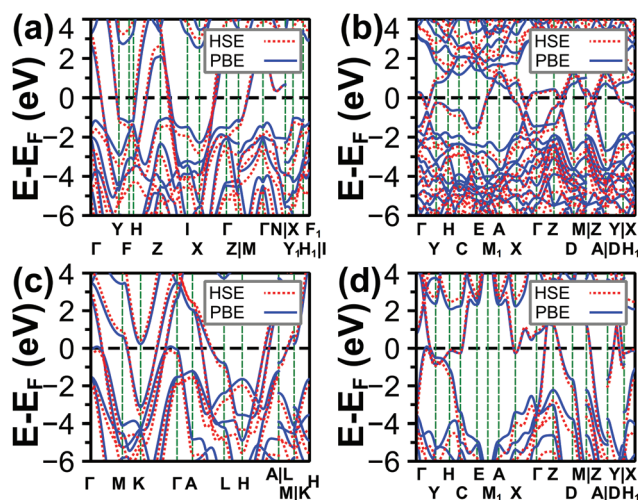


Fig. 3 Band structures of (a) δ_6 -B₆, (b) α -B₁₆, (c) β_{12} -B₅ and (d) δ_3 -B₄ allotropes at PBE and HSE06 levels.

boron crystals, which are semiconductors with significant band gaps.^{5–7} As shown in Fig. S7,† generally speaking, s orbitals make little contribution to the transport, while p orbitals parallel and perpendicular to the basal plane of precursor borophenes make major contributions. The conductivity of the proposed allotropes would be better than that of α -Ga due to their relatively higher values of DOS at the Fermi level (N_F).³⁶

As is well known, higher DOS (N_F) and higher Debye temperature (θ_D) both are beneficial for higher superconducting critical temperatures.⁷⁴ Furthermore, several monolayer borophenes (e.g. δ_6 and β_{12}) were predicted to exhibit intrinsic phonon-mediated superconductivity with critical temperatures of about 10–20 K.¹⁹ In the present study, the superconducting properties of the proposed allotropes are investigated using the Bardeen–Cooper–Schrieffer (BSC) theory⁵¹ and Migdal–Eliashberg theory^{52,53} implemented in the Quantum ESPRESSO package.^{54,55} The critical temperatures T_c are estimated by Allán–Dynes modified McMillan’s approximation of the Eliashberg equation:^{74,75}

$$T_c = \frac{\omega_{\log}}{1.2} \exp \left[-\frac{1.04(1 + \lambda)}{\lambda - \mu_c^*(1 + 0.62\lambda)} \right]$$

where μ_c^* is the effective screened Coulomb repulsion constant (typically ~ 0.1),⁷⁶ λ is the total electron–phonon coupling strength computed from the frequency-dependent Eliashberg spectral function and ω_{\log} is the logarithmic average of frequency.

Our calculated electron–phonon coupling (EPC) constants for δ_6 -B₆, β_{12} -B₅ and δ_3 -B₄ allotropes are 0.52, 0.53 and 0.46 (Fig. 4 and Table S1†), respectively, which are reasonably strong EPC for normal s–p metals and much larger than that

of the α -Ga phase (0.38 at 160 GPa).⁷⁷ The EPC constant for α -B₁₆ is not calculated due to its much lower Debye temperature and much larger cell. The superconducting critical temperatures for δ_6 -B₆, β_{12} -B₅ and δ_3 -B₄ allotropes are estimated to be 10.15, 9.36 and 5.65 K (Table 1 and Table S1†), a little lower than that of β_{12} monolayer borophene (~ 16 K),¹⁹ but higher than those of most superconducting elemental solids.⁷⁸ They are classified as abnormal superconductors⁷⁹ with critical temperatures lower than corresponding monolayer allotropes.⁸⁰ Given the positive dependence of critical temperature on the pressure in a high-pressure bulk boron allotrope,³⁷ the superconductivities of the proposed allotropes may be enhanced under high pressure. For example, the critical temperature of the β_{12} -B₅ phase increased by about 4 K under 100 Gpa (Table S1†). The calculated Eliashberg spectral functions $\alpha^2F(\omega)$ free of pressure are shown in Fig. 4, which was rather unevenly distributed over the frequency for the allotropes. The phonon branches with ω_{qv} between 200 and 800 cm^{-1} contributed about 90% of the EPC of our proposed allotropes. In contrast, about half of the EPC of the monolayer β_{12} borophene came from low-frequency phonons $\omega_{qv} < 200 \text{ cm}^{-1}$,¹⁹ which made negligible contributions to our proposed allotropes. Furthermore, the higher frequency optical branches with out-of-plane A_g and in-plane B_g modes for the δ_6 -B₆, in-plane A'_1 mode for β_{12} -B₅, and out-of-plane A_g mode for δ_3 -B₄ have significant EPC at Γ point (Fig. S8†).

To further understand the geometries and properties of these allotropes, electron localization function (ELF)⁸¹ and solid state adaptive natural density partitioning (SSAdNDP)⁸² were carried out for the proposed allotropes. As shown in Fig. S9a–c,† there are only σ bonds (i.e., 2c–2e, 3c–2e or 5c–2e) in these allotropes, which agrees well with their electronic localization function (ELF) analyses. It may be the reason for their high bulk modulus and Debye temperatures. Compared to δ_3 -B₄, both δ_6 -B₆ and β_{12} -B₅ had additional more delocalized 5c–2e bonds, which may account for their higher critical temperatures. The lack of contribution from π electrons may be the reason why their critical temperatures were lower than monolayer β_{12} borophene⁸³ and MgB₂ bulk.⁸⁴ Bilayer blocks for δ_6 -B₆, β_{12} -B₅ and α -B₁₆ allotropes were connected by 2c–2e bonds between positively charged boron atoms (Fig. S9†) with bond orders of 0.80–0.85 from density derived electrostatic and chemical (DDEC6) atomic population analysis,⁸⁵ while the bilayer blocks for δ_3 -B₄ allotrope were linked by two 3c–2e bonds.

Infrared (IR) spectroscopy is widely used to identify a phase from other allotropes in experiments, so the vibration properties for the proposed allotropes are simulated. As shown in Fig. 5a, the most characteristic IR peaks of the proposed allotropes locate at 679.70 cm^{-1} (B_u), 994.63 cm^{-1} (B_u), 660.22 cm^{-1} (A''_2) and 912.91 cm^{-1} (A_u), respectively, the vibrational modes for which are labeled near their peaks. Besides IR spectroscopy, X-ray diffraction (XRD) patterns were also often used to distinguish allotropes. The XRD patterns were collected and all the peaks were indexed with interplanar distances for ease of comparison with experiments. As shown

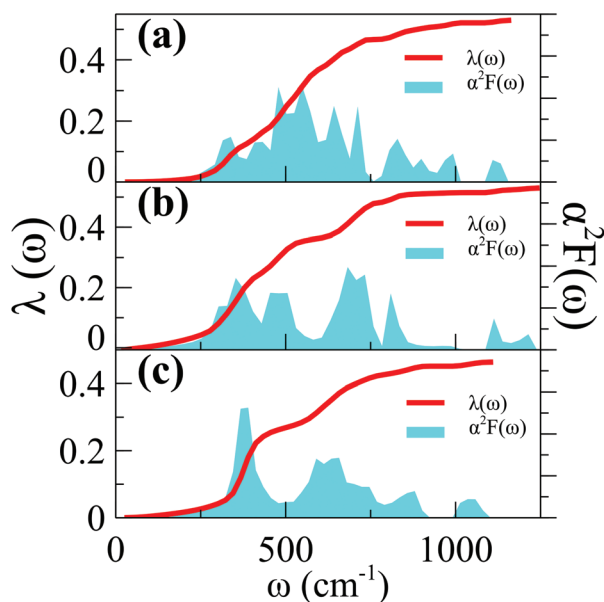


Fig. 4 Calculated Eliashberg spectral functions $\alpha^2F(\omega)$ and cumulative frequency-dependent electron–phonon coupling $\lambda(\omega)$ for (a) δ_6 -B₆, (b) β_{12} -B₅ and (c) δ_3 -B₄ allotropes.

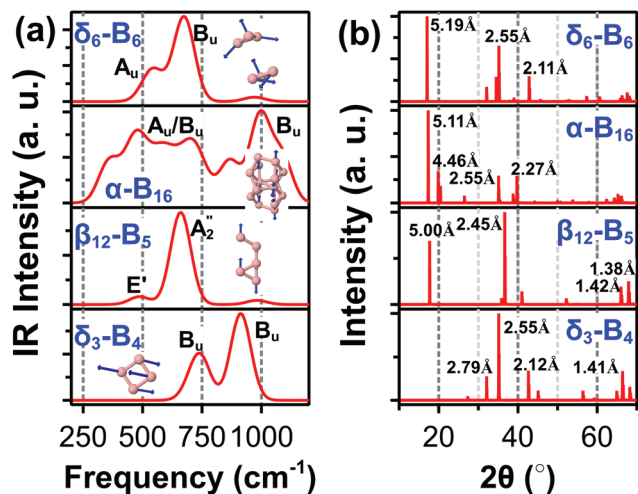


Fig. 5 Simulated (a) infrared (IR) spectroscopy and (b) X-ray diffraction (XRD) patterns of the proposed allotropes. The symmetries for two highest IR peaks and vibrational modes for the highest IR peak are presented. The interplanar distance for typical XRD peaks were also labeled.

in Fig. 5b, all the proposed allotropes have significant peaks with interplanar distances of about 5.0–5.2 Å and 2.45–2.55 Å except $\delta_3\text{-B}_4$, which does not have significant peaks with interplanar distances larger than 3.26 Å.

4. Conclusion

In summary, four novel boron crystals were proposed by staking experimentally realized borophenes with different hole densities. Phonon dispersion curvatures confirmed their kinetic stabilities, and BOMD simulations suggested that all the proposed allotropes were able to withstand high temperatures up to 1000 K, which confirmed their high thermodynamic stabilities. These allotropes were also mechanically stable. Our proposed allotropes are more stable than the boron $\alpha\text{-Ga}$ phase below 1000 K at ambient pressure, and most of them would become more stable than $\alpha\text{-rh}$ or $\gamma\text{-B}_{28}$ phases at appropriate pressure. All the proposed allotropes are metallic in contrast to the semiconducting behaviors of typical boron crystals, due to their quite different construction modes. The multi-center σ bonding accounts for their high bulk modulus and Debye temperatures. Bilayer borophenes with a strong inter-layer bonding tend to act as building blocks of 3D crystals and are connected by $2c\text{-}2e/3c\text{-}2e$ bonds. More importantly, our calculations showed that three of the proposed crystals are superconductors with critical temperatures of about 5–10 K, higher than those of most superconducting elemental solids. Infrared (IR) spectroscopy and X-ray diffraction (XRD) patterns were simulated for the ease of recognition of these allotropes in experiments. Our study suggests a novel preparation method for metallic and superconducting boron solid dispending with high pressure.

Conflicts of interest

There are no conflicts of interest to declare.

Acknowledgements

This work was supported by the National Natural Science Foundation of China (No. 11504213, 21720102006 and 21803037) and the Fund for Shanxi “1331 Project” Key Innovative Research Team (1331KIRT). We greatly acknowledge the computing resources provided by the high performance computing platform of Shanxi University and Hongzhiwei Technology.

References

- 1 L. V. McCarty, J. S. Kasper, F. H. Horn, B. F. Decker and A. E. Newkirk, *J. Am. Chem. Soc.*, 1958, **80**, 2592–2592.
- 2 J. L. Hoard, D. B. Sullenger, C. H. L. Kennard and R. E. Hughes, *J. Solid State Chem.*, 1970, **1**, 268–277.
- 3 C. P. Talley, S. La Placa and B. Post, *Acta Crystallogr.*, 1960, **13**, 271–272.
- 4 R. H. Wentorf, *Science*, 1965, **147**, 49–50.
- 5 A. R. Oganov, J. Chen, C. Gatti, Y. Ma, Y. Ma, C. W. Glass, Z. Liu, T. Yu, O. O. Kurakevych and V. L. Solozhenko, *Nature*, 2009, **457**, 863–867.
- 6 W. Hayami, *J. Solid State Chem.*, 2015, **221**, 378–383.
- 7 T. Ogitsu, E. Schwegler and G. Galli, *Chem. Rev.*, 2013, **113**, 3425–3449.
- 8 A. K. Singh, A. Sadrzadeh and B. I. Yakobson, *Nano Lett.*, 2008, **8**, 1314–1317.
- 9 X. Yang, Y. Ding and J. Ni, *Phys. Rev. B: Condens. Matter Mater. Phys.*, 2008, **77**, 041402.
- 10 Z. A. Piazza, H. S. Hu, W. L. Li, Y. F. Zhao, J. Li and L. S. Wang, *Nat. Commun.*, 2014, **5**, 3113.
- 11 B. Feng, J. Zhang, Q. Zhong, W. Li, S. Li, H. Li, P. Cheng, S. Meng, L. Chen and K. Wu, *Nat. Chem.*, 2016, **8**, 563–568.
- 12 W. Li, L. Kong, C. Chen, J. Gou, S. Sheng, W. Zhang, H. Li, L. Chen, P. Cheng and K. Wu, *Sci. Bull.*, 2018, **63**, 282–286.
- 13 X. Wu, J. Dai, Y. Zhao, Z. Zhuo, J. Yang and X. C. Zeng, *ACS Nano*, 2012, **6**, 7443–7453.
- 14 H. Lu and S.-D. Li, *J. Chem. Phys.*, 2013, **139**, 224307.
- 15 Y. Mu, Q. Chen, N. Chen, H.-G. Lu and S.-D. Li, *Phys. Chem. Chem. Phys.*, 2017, **19**, 19890–19895.
- 16 S.-G. Xu, X.-T. Li, Y.-J. Zhao, J.-H. Liao, W.-P. Xu, X.-B. Yang and H. Xu, *J. Am. Chem. Soc.*, 2017, **139**, 17233–17236.
- 17 X. Zhang, J. Hu, Y. Cheng, H. Y. Yang, Y. Yao and S. A. Yang, *Nanoscale*, 2016, **8**, 15340–15347.
- 18 C. Cheng, J.-T. Sun, H. Liu, H.-X. Fu, J. Zhang, X.-R. Chen and S. Meng, *2D Mater.*, 2017, **4**, 025032.
- 19 E. S. Penev, A. Kutana and B. I. Yakobson, *Nano Lett.*, 2016, **16**, 2522–2526.
- 20 Z. Zhang, Y. Yang, E. S. Penev and B. I. Yakobson, *Adv. Funct. Mater.*, 2017, **27**, 1605059.

- 21 C. Ling, L. Shi, Y. Ouyang, X. C. Zeng and J. Wang, *Nano Lett.*, 2017, **17**, 5133–5139.
- 22 Z. Zhang, E. S. Penev and B. I. Yakobson, *Chem. Soc. Rev.*, 2017, **46**, 6746–6763.
- 23 K. S. Novoselov, A. K. Geim, S. V. Morozov, D. Jiang, Y. Zhang, S. V. Dubonos, I. V. Grigorieva and A. A. Firsov, *Science*, 2004, **306**, 666–669.
- 24 A. J. Mannix, X.-F. Zhou, B. Kiraly, J. D. Wood, D. Alducin, B. D. Myers, X. Liu, B. L. Fisher, U. Santiago, J. R. Guest, M. J. Yacaman, A. Ponce, A. R. Oganov, M. C. Hersam and N. P. Guisinger, *Science*, 2015, **350**, 1513–1516.
- 25 R. Wu, I. K. Drozdov, S. Eltinge, P. Zahl, S. Ismail-Beigi, I. Božović and A. Gozar, *Nat. Nanotechnol.*, 2018, **14**, 44–49.
- 26 B. Kiraly, X. Liu, L. Wang, Z. Zhang, A. J. Mannix, B. L. Fisher, B. I. Yakobson, M. C. Hersam and N. P. Guisinger, *ACS Nano*, 2019, **13**, 3816–3822.
- 27 L. Liu, Z. Zhang, X. Liu, X. Xuan, B. I. Yakobson, M. C. Hersam and W. Guo, *Nano Lett.*, 2020, **20**, 1315–1321.
- 28 C. Chen, H. Lv, P. Zhang, Z. Zhuo, Y. Wang, C. Ma, W. Li, X. Wang, B. Feng, P. Cheng, X. Wu, K. Wu and L. Chen, *Nat. Chem.*, 2022, **14**, 25–31.
- 29 X. Liu, Q. Li, Q. Ruan, M. S. Rahn, B. I. Yakobson and M. C. Hersam, *Nat. Mater.*, 2022, **21**, 35–40.
- 30 Y. Xu, X. Xuan, T. Yang, Z. Zhang, S.-D. Li and W. Guo, *Nano Lett.*, 2022, **22**, 3488–3494.
- 31 Z. Zhang, A. J. Mannix, X. Liu, Z. Hu, N. P. Guisinger, M. C. Hersam and B. I. Yakobson, *Sci. Adv.*, 2019, **5**, eaax0246.
- 32 Y. Mu and S.-D. Li, *J. Phys. Chem. C*, 2020, **124**, 28145–28151.
- 33 Q. Li, V. S. C. Kolluru, M. S. Rahn, E. Schwenker, S. Li, R. G. Hennig, P. Darancet, M. K. Y. Chan and M. C. Hersam, *Science*, 2021, **371**, 1143–1148.
- 34 G. Ferlat, A. P. Seitsonen, M. Lazzeri and F. Mauri, *Nat. Mater.*, 2012, **11**, 925–929.
- 35 H. Lin, H. Shi, Z. Wang, Y. Mu, S. Li, J. Zhao, J. Guo, B. Yang, Z.-S. Wu and F. Liu, *ACS Nano*, 2021, **15**, 17327–17336.
- 36 U. Häussermann, S. I. Simak, R. Ahuja and B. Johansson, *Phys. Rev. Lett.*, 2003, **90**, 065701.
- 37 M. I. Eremets, *Science*, 2001, **293**, 272–274.
- 38 G. Kresse and J. Furthmüller, *Phys. Rev. B: Condens. Matter Mater. Phys.*, 1996, **54**, 11169–11186.
- 39 G. Kresse and J. Hafner, *J. Phys.: Condens. Matter*, 1994, **6**, 8245–8257.
- 40 P. E. Blochl, *Phys. Rev. B: Condens. Matter Mater. Phys.*, 1994, **50**, 17953–17979.
- 41 G. Kresse and D. Joubert, *Phys. Rev. B: Condens. Matter Mater. Phys.*, 1999, **59**, 1758–1775.
- 42 J. P. Perdew, K. Burke and M. Ernzerhof, *Phys. Rev. Lett.*, 1996, **77**, 3865–3868.
- 43 H. J. Monkhorst and J. D. Pack, *Phys. Rev. B: Solid State*, 1976, **13**, 5188–5192.
- 44 S. Curtarolo, W. Setyawan, G. L. W. Hart, M. Jahnatek, R. V. Chepulskii, R. H. Taylor, S. Wang, J. Xue, K. Yang, O. Levy, M. J. Mehl, H. T. Stokes, D. O. Demchenko and D. Morgan, *Comput. Mater. Sci.*, 2012, **58**, 218–226.
- 45 S. Grimme, J. Antony, S. Ehrlich and H. Krieg, *J. Chem. Phys.*, 2010, **132**, 154104.
- 46 S. Grimme, S. Ehrlich and L. Goerigk, *J. Comput. Chem.*, 2011, **32**, 1456–1465.
- 47 A. V. Krukau, O. A. Vydrov, A. F. Izmaylov and G. E. Scuseria, *J. Chem. Phys.*, 2006, **125**, 224106–224105.
- 48 A. Togo, F. Oba and I. Tanaka, *Phys. Rev. B: Condens. Matter Mater. Phys.*, 2008, **78**, 134106.
- 49 K. Momma and F. Izumi, *J. Appl. Crystallogr.*, 2011, **44**, 1272–1276.
- 50 R. Hill, *Proc. Phys. Soc., London, Sect. A*, 1952, **65**, 349–354.
- 51 J. Bardeen, L. N. Cooper and J. R. Schrieffer, *Phys. Rev.*, 1957, **108**, 1175–1204.
- 52 A. B. Migdal, *Sov. Phys. JETP*, 1958, **7**, 996–1001.
- 53 G. M. Eliashberg, *Sov. Phys. JETP*, 1960, **11**, 696–702.
- 54 P. Giannozzi, S. Baroni, N. Bonini, M. Calandra, R. Car, C. Cavazzoni, D. Ceresoli, G. L. Chiarotti, M. Cococcioni, I. Dabo, *et al.*, *J. Phys.: Condens. Matter.*, 2009, **21**, 395502.
- 55 P. Giannozzi, O. Andreussi, T. Brumme, O. Bunau, M. B. Nardelli, M. Calandra, R. Car, C. Cavazzoni, D. Ceresoli, M. Cococcioni, N. Colonna, I. Carnimeo, A. D. Corso, S. de Gironcoli, P. Delugas, R. A. D. Jr, A. Ferretti, A. Floris, G. Fratesi, G. Fugallo, R. Gebauer, U. Gerstmann, F. Giustino, T. Gorni, J. Jia, M. Kawamura, H.-Y. Ko, A. Kokalj, E. Küçükbenli, M. Lazzeri, M. Marsili, N. Marzari, F. Mauri, N. L. Nguyen, H.-V. Nguyen, A. O.-d. la-Roza, L. Paulatto, S. Poncé, D. Rocca, R. Sabatini, B. Santra, M. Schlipf, A. P. Seitsonen, A. Smogunov, I. Timrov, T. Thonhauser, P. Umari, N. Vast, X. Wu and S. Baroni, *J. Phys.: Condens. Matter*, 2017, **29**, 465901.
- 56 D. R. Hamann, *Phys. Rev. B: Condens. Matter Mater. Phys.*, 2013, **88**, 085117.
- 57 E. Amberger and W. Stumpf, *Gmelin Handbook of Inorganic and Organometallic Chemistry*, Springer-Verlag, Berlin, 1981.
- 58 V. L. Solozhenko, O. O. Kurakevych and A. R. Oganov, *J. Superhard Mater.*, 2008, **30**, 428–429.
- 59 G. A. Slack, D. W. Oliver and F. H. Horn, *Phys. Rev. B: Solid State*, 1971, **4**, 1714–1720.
- 60 H. Tang and S. Ismail-Beigi, *Phys. Rev. Lett.*, 2007, **99**, 115501.
- 61 H. Shu, F. Li, P. Liang and X. Chen, *Nanoscale*, 2016, **8**, 16284–16291.
- 62 Z. Zhang, Y. Yang, G. Gao and B. I. Yakobson, *Angew. Chem., Int. Ed.*, 2015, **54**, 13022–13026.
- 63 Q. Zhong, J. Zhang, P. Cheng, B. Feng, W. Li, S. Sheng, H. Li, S. Meng, L. Chen and K. Wu, *J. Phys.: Condens. Matter.*, 2017, **29**, 095002.
- 64 D. Z. Li, Q. Chen, Y. B. Wu, H. G. Lu and S. D. Li, *Phys. Chem. Chem. Phys.*, 2012, **14**, 14769–14774.
- 65 N. Karmodak and E. D. Jemmis, *J. Phys. Chem. C*, 2018, **122**, 2268–2274.
- 66 D. Sheppard, P. Xiao, W. Chemelewski, D. D. Johnson and G. Henkelman, *J. Chem. Phys.*, 2012, **136**, 074103.
- 67 X.-Q. Chen, H. Niu, D. Li and Y. Li, *Intermetallics*, 2011, **19**, 1275–1281.

- 68 S. F. Pugh, *Philos. Mag.*, 1954, **45**, 823–843.
- 69 I. N. Frantsevich, F. F. Voronov and S. A. Bokuta, *Elastic Constants and Elastic Moduli of Metals and Insulators: Handbook*, Naukova dumka, Kiev, 1982.
- 70 Z.-j. Wu, E.-j. Zhao, H.-p. Xiang, X.-f. Hao, X.-j. Liu and J. Meng, *Phys. Rev. B: Condens. Matter Mater. Phys.*, 2007, **76**, 054115.
- 71 F. Mouhat and F.-X. Coudert, *Phys. Rev. B: Condens. Matter Mater. Phys.*, 2014, **90**, 224104.
- 72 O. L. Anderson, *J. Phys. Chem. Solids*, 1963, **24**, 909–917.
- 73 C. Wolverton and A. Zunger, *Phys. Rev. B: Condens. Matter Mater. Phys.*, 1995, **52**, 8813–8828.
- 74 W. L. McMillan, *Phys. Rev.*, 1968, **167**, 331–344.
- 75 P. B. Allen and R. C. Dynes, *Phys. Rev. B: Condens. Matter Mater. Phys.*, 1975, **12**, 905–922.
- 76 C. F. Richardson and N. W. Ashcroft, *Phys. Rev. Lett.*, 1997, **78**, 118–121.
- 77 Y. Ma, J. S. Tse, D. D. Klug and R. Ahuja, *Phys. Rev. B: Condens. Matter Mater. Phys.*, 2004, **70**, 214107.
- 78 J. A. Flores-Livas, L. Boeri, A. Sanna, G. Profeta, R. Arita and M. Eremets, *Phys. Rep.*, 2020, **856**, 1–78.
- 79 E. Navarro-Moratalla, J. O. Island, S. Mañas-Valero, E. Pinilla-Cienfuegos, A. Castellanos-Gomez, J. Quereda, G. Rubio-Bollinger, L. Chirolli, J. A. Silva-Guillén, N. Agraït, G. A. Steele, F. Guinea, H. S. J. van der Zant and E. Coronado, *Nat. Commun.*, 2016, **7**, 11043.
- 80 Y. Zhao, S. Zeng and J. Ni, *Appl. Phys. Lett.*, 2016, **108**, 242601.
- 81 A. D. Becke and K. E. Edgecombe, *J. Chem. Phys.*, 1990, **92**, 5397–5403.
- 82 T. R. Galeev, B. D. Dunnington, J. R. Schmidt and A. I. Boldyrev, *Phys. Chem. Chem. Phys.*, 2013, **15**, 5022–5029.
- 83 Y. Zhao, S. Zeng, C. Lian, Z. Dai, S. Meng and J. Ni, *Phys. Rev. B*, 2018, **98**, 134514.
- 84 H. J. Choi, D. Roundy, H. Sun, M. L. Cohen and S. G. Louie, *Nature*, 2002, **418**, 758–760.
- 85 T. A. Manz, *RSC Adv.*, 2017, **7**, 45552–45581.